HHS Public Access

Author manuscript

J Bone Miner Res. Author manuscript; available in PMC 2021 July 01.

Published in final edited form as:

J Bone Miner Res. 2020 July ; 35(7): 1274–1281. doi:10.1002/jbmr.4005.

Changes in Skeletal Microstructure Through Four Continuous Years of rhPTH(1-84) Therapy in Hypoparathyroidism

Natalie E. Cusano[1], **Mishaela R. Rubin**[2], **John M. Williams**[2], **Sanchita Agarwal**[2], **Gaia Tabacco**[3], **Donovan Tay**[4], **Rukshana Majeed**[2], **Beatriz Omeragic**[2], **John P. Bilezikian**[2]

[1]Department of Medicine, Division of Endocrinology, Lenox Hill Hospital, New York, NY

[2]Department of Medicine, Division of Endocrinology, College of Physicians & Surgeons, Columbia University, New York, NY

[3]Unit of Endocrinology and Diabetes, Department of Medicine, University Campus Bio-Medico, Rome, Italy

[4]Department of Medicine, Sengkang General Hospital, Singapore

Abstract

Bone remodeling is reduced in hypoparathyroidism, resulting in increased areal bone mineral density (BMD) by dual energy X-ray absorptiometry (DXA) and abnormal skeletal indices by transiliac bone biopsy. We have now studied skeletal microstructure by high resolution peripheral quantitative computed tomography (HRpQCT) through 4 years of treatment with recombinant human PTH(1–84) [rhPTH(1–84)] in 33 patients with hypoparathyroidism (19 with postsurgical disease, 14 idiopathic). We calculated Z-scores for our cohort compared to previously published normative values. We report results at baseline and 1, 2, and 4 years of continuous therapy with rhPTH(1–84). The majority of patients (62%) took rhPTH(1–84) 100 μg every other day for the majority of the 4 years. At 48 months, areal bone density increased at the lumbar spine (+4.9 ± 0.9%) and femoral neck (+2.4 ± 0.9%), with declines at the total hip (−2.3 ± 0.8%) and ultradistal radius (−2.1 ± 0.7%) ($p<0.05$ for all). By HRpQCT, at the radius site, very similar to the ultradistal DXA site, total volumetric BMD declined from baseline but remained above normative values at 48 months (Z-score +0.56). Cortical volumetric BMD was lower than normative controls at baseline at the radius and tibia (Z-scores −1.28 and −1.69, respectively), and further declined at 48 months (−2.13 and −2.56, respectively). Cortical porosity was higher than normative controls at baseline at the tibia (Z-score +0.72) and increased through 48 months of therapy at both sites (Z-scores +1.80 and +1.40, respectively). Failure load declined from baseline at both the radius and tibia, although remained higher than normative controls at 48 months (Z-scores +1.71 and +1.17, respectively). This is the first report of noninvasive high-resolution imaging in a cohort of hypoparathyroid patients treated with any PTH therapy for this length of time. The results give insights into the effects of long-term rhPTH(1–84) in hypoparathyroidism.

Corresponding author: John P. Bilezikian, MD, PhD (hon), Department of Medicine, PH 8E-105G, Columbia University College of Physicians & Surgeons, 630 West 168th Street, New York, NY 10032, Phone: (212) 305-6257, Fax: (212) 305-8466, jpb2@cumc.columbia.edu.

Authors' roles: Study design: MRR and JPB. Study conduct: NEC, MRR, and JPB. Data collection: NEC, MRR, SA, RM, and BO. Data analysis: NEC, JW, and SA. Data interpretation: NEC, SA, and JPB. Drafting manuscript: NEC. Revising manuscript content (all authors). Approving final version of manuscript (all authors).

Keywords

Hypoparathyroidism; high resolution peripheral quantitative computed tomography; HRpQCT; HR pQCT; bone microarchitecture

Introduction

Hypoparathyroidism is a disorder characterized by hypocalcemia and deficient or absent circulating levels of parathyroid hormone (PTH). Areal bone mineral density (BMD) in hypoparathyroid patients is generally above average for euparathyroid controls, and bone turnover is markedly reduced.[1–5] We previously reported our findings using high resolution peripheral quantitative computed tomography (HRpQCT) and finite element analysis (FEA) to study bone geometry, microarchitecture and strength in a cohort of patients with hypoparathyroidism treated with conventional therapy.[6] We demonstrated abnormalities in both the cortical and trabecular compartments.

Histomorphometric analysis of iliac crest bone biopsy specimens in hypoparathyroid patients demonstrates abnormal structural and dynamic skeletal parameters in patients treated with conventional therapy and has shown that rhPTH(1–84) can improve abnormally low bone turnover and restore skeletal parameters indices towards a more euparathyroid state.[2,3,7] We now report results using a noninvasive high-resolution imaging technology in hypoparathyroid patients at baseline and 1, 2, and 4 years after starting rhPTH(1–84) therapy.

Materials and Methods

Hypoparathyroid subjects

Patients were diagnosed with hypoparathyroidism in the setting of hypocalcemia and undetectable or insufficient concentrations of PTH requiring supplemental calcium and/or active vitamin D to maintain serum calcium levels in the low normal range. Hypoparathyroidism was present for at least one year to document a chronic hypoparathyroid state. Patients were excluded if they had ever received therapy with PTH(1–34) or rhPTH(1–84) prior to study entry. The present cohort includes patients who completed therapy with rhPTH(1–84) through four years as part of our study protocol and includes patients from previously published cohorts.[6,8] Baseline imaging of the radius was considered to be inadequate in two patients; they were excluded from post-treatment analysis at this site.

Patients were identified and recruited from the Metabolic Bone Diseases Unit of Columbia University Medical Center (CUMC) and from the Hypoparathyroidism Association. The study was approved by the Institutional Review Board of CUMC. All subjects gave written informed consent.

Control population

We utilized previously published HRpQCT normative data from the Calgary, Alberta cohort of the Canadian Multicentre Osteoporosis Study (CaMos).[9] CaMos is a 10-year prospective population-based study of over 9000 men and women living within 50 km of nine Canadian cities, originally recruited between 1997 and 1998 using a stratified random-sampling technique.[10] At the 10-year follow-up visit, subjects were invited to participate in a HRpQCT substudy. For this analysis, we used the published data for men (n=274) and women (n=592) aged 16 to 98 years, providing age-, sex-, and site-specific centiles for HRpQCT parameters.[11] We chose to use the CaMos reference data as it provides a population-based North American cohort with data from both the radius and tibia, including estimates of bone strength. Our analyses for cortical and trabecular microarchitecture, failure load, and estimated bone strength are identical to those used for the CaMos data.[11]

Biochemical evaluation

The baseline calcium value represents the average of up to three pre-treatment serum calcium determinations. Biochemical indices were measured by automated techniques. The normal ranges for all assays are provided in Table 1.

Imaging evaluation

Areal BMD—Areal BMD was evaluated at the lumbar spine (L1-L4), total hip, femoral neck, 1/3 and ultradistal radius using dual energy X-ray absorptiometry (DXA; Hologic QDR4500, Waltham, MA). Patients were measured on the same densitometer, using the same software, scan speed, and technologist, certified by the International Society of Clinical Densitometry. Measurements were performed twice at baseline for most subjects, with the average value of the two BMD measurements used for the baseline value. Short-term *in vivo* precision error (root-mean-square standard deviation) was 0.026 g/cm^2 for L1-L4 (1.1%), 0.041 g/cm^2 for the femoral neck (2.4%), and 0.033 g/cm^2 (1.8%) for the forearm. Areal BMD was compared to a healthy population from the National Health and Nutrition Examination Survey provided by the Hologic software.

Volumetric BMD and microarchitecture—The nondominant distal radius and tibia were evaluated using HRpQCT (Xtreme CT; Scanco Medical AG, Brüttisellen, Switzerland) with a standard protocol (60 kVp, 900 μA, and 100-ms integration time) with a nominal isotropic resolution of 82 μm.[12] The region of interest was defined using an antero-posterior scout view wherein a reference line was manually placed at the distal end plate of the radius and tibia. At the radius, the first of 110 parallel CT slices was acquired 9.5 mm proximal to the reference line and at the tibia 22.5 mm proximal to the reference line. Attenuation data were converted to equivalent hydroxyapatite (HA) densities. The manufacturer phantom was scanned daily for quality control.

The protocol used for image analysis has been previously described and validated.[9,12–15] Briefly, the volume of interest was separated using a semi-automated threshold-based algorithm into cortical and trabecular compartments. Total and trabecular bone density (Tt.BMD, Tb.BMD, mg HA/cm^3) measurements were obtained. Trabecular bone volume (BV/TV, %) was derived from Tb.BMD using the assumption that fully mineralized bone

has a density of 1,200 mg HA/cm^3 [BV/TV %= 100 × (Tb.BMD/1200)]. Trabecular number (Tb.N, 1/mm) was defined as the inverse of the mean spacing of the mid-axes. Trabecular thickness (Tb.Th, mm) and trabecular separation (Tb.Sp, mm) were derived from BV/TV and Tb.N using standard morphologic relationships [Tb.Th=(BV/TV)/Tb.N, Tb.Sp=(BV/TV)/Tb.N]. Short-term *in vivo* precision error at our facility is 0.7–1.5% for total and trabecular densities and 2.5–4.4% for all trabecular microarchitectural parameters.

In addition to the standard morphologic analysis above, we used an automated segmentation algorithm [Image Processing Language (IPL, Version 5.08b, Scanco Medical)] to measure total and cortical bone cross-sectional areas (Tt.Ar, Ct.Ar, mm^2), cortical porosity (Ct.Po, %), cortical thickness (Ct.Th, mm) and cortical density (Ct.BMD, mm HA/cm^3). Ct.Po was defined by the number of void voxels in each thresholded cortex image divided by the total number of cortical voxels. Ct.Th was determined using a distance transform after removing the intracortical pores. Ct.BMD was calculated by the average mineral density in the region demarcated by the autosegmentation cortical bone mask. The precision error for the automated segmentation algorithm is <1.5%.[16] This methodological approach, at this time, is not able to examine the subcompartmentization of cortical bone.

Finite element analysis—The image analysis used has been previously described and validated.[9,17,18] Whole-bone HRpQCT images of the radius and tibia were converted into finite-element models (FAIM, Version 8.0, Numerics88, Calgary, Canada) to estimate whole-bone stiffness (N/mm), defined as the reaction force calculated by the model at 1% strain divided by the average cross-sectional area from the morphological analysis. The *in vivo* precision error for the stiffness measure is <3.5%.[19] Failure load (N) was calculated using the Pistoia criterion.[20]

Statistical analysis

Descriptive characteristics of study patients were tabulated for continuous variables by means and standard deviations or medians with interquartile ranges. A linear mixed model for repeated measures approach was applied to study percentage change in all patients at 1, 2, and 4 years. We used linear regression to assess the contribution of age, gender, and duration of hypoparathyroidism to HRpQCT variables and estimated bone strength in our hypoparathyroid patients. We calculated Z-scores for HRpQCT variables and failure load for our hypoparathyroid patients compared to normative data from CaMos.[11] T-tests were used to compare Z-scores to 0. All statistical tests were performed at the level of significance of 0.05. Statistical analyses were performed using R version 3.5.1.[21]

Results

Baseline characteristics

The mean age of the hypoparathyroid patients was 47 ± 14 years (range 26–72) with the cohort comprised of 73% women, consistent with the demographics of the disease (Table 1). The two etiologies of hypoparathyroidism were surgical (19 patients) and idiopathic (14 patients). One of the postsurgical postmenopausal women had a prior diagnosis of primary hyperparathyroidism and had experienced at least 3 years of hypoparathyroidism following

parathyroid resection. The remaining patients were status post thyroid surgery for benign or malignant disease. The median known duration of hypoparathyroidism was 6 years [interquartile range (IQR) 3, 17], with a range of 2–45 years.

Treatment with rhPTH(1–84)

Patients were initially treated with rhPTH(1–84) at a dose of 100 μg every other day due to a pilot study that demonstrated improvement in biochemical markers of bone turnover with this regimen.[22] Dosage adjustments were made when alternative dosing regimens of 25, 50, and 75 μg became available. The majority of patients (62%) were treated with 100 μg every other day for the majority of the 4 years. The median length of treatment with rhPTH(1–84) 100 μg every other day was 33 months (IQR 12, 42). At the end of the study, the dosages of rhPTH(1–84) were: 25 μg daily (n=2), 50 μg daily (n=19), 75 μg daily (n=3), 100 μg daily (n=4), 100 μg every other day (n=4), 100 μg every 3 days (n=1). The median daily dose at 48 months was 50 μg (IQR 50, 50).

Calcium supplementation declined by 36% from baseline to 48 months on rhPTH(1–84) therapy [from median 1833 to 1689 mg (IQR 600, 2000 mg); p=0.005] and calcitriol supplementation declined by 64% (from median 0.50 to 0.25 μg (IQR 0.00, 0.50 μg); p<0.001]. No fractures occurred during the study period.

Biochemical evaluation

Serum calcium concentration at baseline was typically normal as a result of supplementation with calcium and active vitamin D (8.7 ± 1.0 mg/dL), and remained overall at goal on rhPTH(1–84) therapy (8.3 ± 0.7 mg/dL). Although median TSH was in the normal range at baseline, it was reduced in 4 subjects having a TSH value <0.1 μIU/L.

Imaging

DXA—Baseline areal BMD values, T- and Z-scores and percentage change from baseline at 1, 2, and 4 years of rhPTH(1–84) therapy are shown in Table 2. At baseline, areal BMD T- and Z-scores were significantly above average at all sites compared to a healthy population. The lumbar spine site showed a significant increase starting at 24 months, with an increase of +4.9 ± 0.9% (p<0.001) at 48 months. Bone density at the femoral neck was increased by +2.4 ± 0.9% (p<0.05) at 48 months. The total hip site declined starting at 24 months, with a fall of −2.3 ± 0.8% (p<0.01) at 48 months. Bone density at the 1/3 and ultradistal radius declined at 12 months, with no significant changes at 24 months, and a significant decline was noted at the ultradistal radius of −2.1 ± 0.7% at 48 months (p<0.01).

HRpQCT—At baseline, at the radius, Ct.Ar, Tt.BMD, and Ct.Th were higher in the hypoparathyroid patients compared to normative controls (Z-scores +0.83, +0.73, +0.94, respectively; p<0.05 for all) (Figure 1A, Table 3). Ct.BMD was lower in the hypoparathyroid patients compared to controls (Z-score −1.28; p<0.001). With rhPTH(1–84) therapy, significant declines were noted in Tt.BMD and Ct.BMD, with declines of −2.9 ± 0.7% and −3.8 ± 0.7% at 48 months, respectively (p<0.001 for both). Ct.Po was increased by +88.5 ± 17.7% at 48 months (p<0.001). At 48 months of rhPTH(1–84) therapy, Ct.Ar, Tt.BMD, and Ct.Th more closely approached the values for normative controls. Ct.Po was increased

relative to normative controls (Z-score +1.80, p<0.0001). Ct.BMD declined further compared to normative controls (Z-score −2.13, p<0.0001).

At baseline, at the tibia, Ct.Ar, Ct.Th, Ct.Po, and Tb.N were higher in the hypoparathyroid patients compared to normative controls (Z-scores +0.57, +0.59, +0.72, +0.52, respectively; p<0.01 for all) (Figure 1B, Table 3). Ct.BMD, Tb.Th, and Tb.Sp were lower in the hypoparathyroid patients compared to controls (Z-scores −1.69, −0.32, and −0.29, respectively; p<0.05 for all). At the tibia, a significant decline was noted in Ct.BMD starting at 24 months. There were declines in Tt.BMD and Ct.BMD at 48 months of −1.9 ± 0.5% and −4.4 ± 0.7%, respectively (p<0.001 for both). Ct.Po increased starting at 24 months, reaching values +23.1 ± 4.8% higher at 48 months (p<0.001). At 48 months of rhPTH(1–84) therapy, Tt.BMD and Ct.Th more closely approached the values for normative controls. Ct.Po remained higher than normative values (Z-score +1.40, p<0.0001). Ct.BMD declined further compared to normative values (Z-score −2.56, p<0.0001). Tb.N, Tb.Th, and Tb.Sp did not significantly change within the cohort but remained different to normative controls at 48 months (Z-scores of +0.67, −0.38, and −0.36, respectively; p<0.05 for all).

FEA—Compared to normative controls, failure load was much greater at both the radius and tibia at baseline (Z-scores +1.94 and +1.35, respectively; p<0.0001 for both) (Figure 1A and 1B, Table 3). At the radius, failure load declined starting at 24 months, with a decline of −2.6 ± 1.0% (p<0.05) at 48 months. There was no significant change in stiffness. At the tibia, stiffness and failure load declined at 48 months by −2.7 ± 0.9% and −2.2 ± 0.8%, respectively (p<0.01 for both). After 48 months of rhPTH(1–84) therapy, failure load remained well above values for normative controls at both the radius and tibia (Z-scores +1.71 and +1.17, respectively; p<0.0001 for both).

Linear regression analysis

In the linear regression model, age had significant effects on Tt.BMD and Ct.BMD at both the radius and tibia. For every 10-year increase in age, there were declines of −1.0% in both parameters at both the radius and tibia (p<0.05 for all). In addition, at the radius, for every 10-year increase in age, Ct.Po was increased by 18.0% (p<0.05). There were no significant effects of gender or disease duration on any of the measured parameters.

Discussion

This is the first investigation to report results using noninvasive high-resolution imaging in a cohort of hypoparathyroid patients treated with any parathyroid hormone therapy for this length of time for any disease. The results provide new insights into PTH-induced changes from a baseline cohort of individuals characterized by PTH deficiency. The abnormal skeletal microstructure characteristic of hypoparathyroidism was tracked in the context of exposure to PTH therapy over time.

Hypoparathyroidism is characterized by markedly decreased bone turnover and increased areal BMD by DXA at the spine and hip compared to euparathyroid individuals.[23–26] Using HRpQCT and FEA, we have reported on bone geometry, microarchitecture and strength in a cohort of patients with hypoparathyroidism on conventional therapy with calcium and active

vitamin D.[6] In that study, we demonstrated microarchitectural differences in both the cortical and trabecular compartments at both the radius and tibia in patients with hypoparathyroidism compared to healthy controls. In the present study, we report longitudinal changes in a subset of these patients completing therapy with rhPTH(1–84) through four years.

There were increases in areal BMD at the spine and femoral neck and declines at the total hip and ultradistal radius associated with rhPTH(1–84) therapy. The 1/3 radius site also declined significantly at 12 months, with a trend towards an increase at 48 months. The hip sites are an admixture of trabecular and cortical bone, and the 1/3 radius site is comprised primarily of cortical bone. While the spine and ultradistal radius are both rich in trabecular bone, loading differences at these two sites could account for site-specific differences with rhPTH(1–84) therapy. Increased mineralization activity could also account, at least in part, for the increase in areal BMD at the spine and femoral neck. It was therefore instructive to consider DXA and HRpQCT values at the same ultradistal radius site. By HRpQCT, total volumetric BMD declined at both the radius and tibia, with declines in cortical, but not trabecular, volumetric bone density. The distinction between trabecular and cortical bone by HRpQCT helps to identify the cortical compartment as the one that is more prone to show declines with PTH therapy while the trabecular compartment is more likely to show the anabolic properties of PTH. It is interesting to note that this proclivity is seen in this disease characterized by classically low bone remodeling, while previous reports have shown the same disposition in primary hyperparathyroidism. Moreover, it seems likely that the increase in bone remodeling as a function of PTH therapy in hypoparathyroidism gives the same net effect as is seen in euparathyroid subjects exposed to PTH on these two compartments.[8,26–28]

Our group previously reported data on skeletal microstructure using histomorphometric analysis of bone biopsy specimens of the iliac crest in hypoparathyroid patients treated with rhPTH(1–84), including some patients from this cohort.[2,7] In the first histomorphometric analysis through two years of rhPTH(1–84) therapy, cortical porosity increased by 24% at 24 months.[2] While cancellous bone volume did not change, trabecular width decreased with rhPTH(1–84) therapy and was no longer different from controls. Trabecular number also increased, primarily due to trabecular tunneling. More recently, we have also demonstrated longer-term data in hypoparathyroid patients treated with an average of eight years of PTH therapy.[7] With these long-term biopsies, there were significant increases in cancellous bone volume of 50% and trabecular number of 39%, surpassing control levels. Cortical porosity also tended to increase by 51%, also surpassing control levels. Our previously published histomorphometric data and the HRpQCT data presented here are consistent with the pharmacological effects of PTH. It would be interesting to see how more physiologic replacement regimens of PTH alter this pharmacological profile of PTH replacement therapy in hypoparathyroidism.

Our prior results demonstrated higher Ct.BMD and lower Ct.Po in patients with hypoparathyroidism compared to 20–29 year-old gender-matched euparathyroid individuals at both the radius and tibia.[6] In the present study, we found that Ct.BMD was lower and Ct.Po higher than normative data that was age- and gender-matched. Values for Ct.BMD in

our subset of hypoparathyroid patients from the previous study were similar. However, the values for the much larger cohort of control patients were overall higher. Because of the difference in values in the control population, our hypoparathyroid patients now had lower Ct.BMD compared to the normative controls. With regard to Ct.Po, the method of Ct.Po measurement was updated between the previous study and the current study, which may account for some of the difference. The values for Ct.Po reported for the CaMos cohort are generally lower than those for other normative cohorts.[29–31] Thus, until this issue of the control population is clarified further, it is our view that our results are best interpreted with regard to changes from baseline values.

Results from the current investigation show that Ct.BMD declines and Ct.Po increases with rhPTH(1–84) therapy. Ct.Po is well known to be associated with the degree of bone remodeling, and would be expected to increase as bone remodeling increases in hypoparathyroid patients treated with PTH therapy. Ct.BMD is proportional to the degree of mineralization and inversely proportional to Ct.Po.[32] The advanced segmentation algorithm we used has been previously validated and demonstrated to be robust in the characterization of cortical features from HRpQCT images in healthy subjects.[33] This analysis, however, did not have the capability to identify whether the overall increase in Ct.Po was confined to specific subcortical compartments of bone or rather was a more generalized effect. Moreover, in view of the likely actions of PTH to influence the partitioning of the cortical and trabecular compartments of bone, the interpretation of these changes in Ct.Po await further more detailed dissection of the microskeletal anatomy of these two compartments under these conditions. For example, the transition zone between cortical and trabecular bone could be a “driving” force in the overall effects attributed either to the cortical or trabecular compartments as they are defined conventionally. Some of the increase in Ct.Po we noted in this study may be more accurately attributable to bone remodeling in the transitional zone. Issues in distinguishing cortical versus trabecular bone in this zone may also be responsible, at least in part, for the lack of any changes in trabecular parameters measured using HRpQCT in this cohort. Studies to examine these possibilities are being conducted at this time. Of note, in a cohort of postmenopausal women with osteoporosis studied using HRpQCT, treatment with 24 months of teriparatide [PTH(1–34)] increased Ct.Po at the radius by 33.0 ± 40.1% and at the tibia by 10.2 ± 12.1% ($p<0.001$ for both), similar to our findings in hypoparathyroid patients at 24 months. The effects of longer-term administration of PTH therapy in euparathyroid individuals has not been studied.[34]

The differences between our HRpQCT results and those from bone biopsy may be attributed to previously reported differences between the iliac crest and other sites.[35] The iliac crest may not necessarily be representative of other skeletal sites. In patients with primary hyperparathyroidism, trabecular microarchitecture is maintained by histomorphometric analysis of bone biopsy specimens of the iliac crest.[36] However, trabecular microarchitectural parameters are decreased using HRpQCT,[37] more consistent with fracture data indicated increased risk of vertebral fracture.[38] Thus, it is our view that as valuable as histomorphometric data are, caution is advised in any attempts to connect this technology with others such as HRpQCT that measure anatomical sites that are more likely to be relevant to sites of skeletal stress and loading.

We also noted significant declines in estimated bone stiffness at the tibia and failure load at both the radius and tibia. The combination of decreased total and cortical volumetric BMD and increased Ct.Po may account for the decrease noted in these FEA parameters. It is of interest that bone stiffness and failure load declined relatively little in comparison to the more evident increase in Ct.Po. Previous studies have emphasized that the relationship between Ct.Po and bone strength is exponential, with small changes in Ct.Po usually resulting in much larger declines in bone strength.[31,39,40] Unfortunately, the FEA models used in this analysis cannot measure differences in tissue mineralization, which has its own beneficial effect on bone strength.[41] While failure load declined significantly, it is important to note it remained above normative values, that is, bone strength continued to be above average. The effect that these declines in estimated bone strength may have on fracture risk in patients with hypoparathyroidism is unknown, especially since more data are needed regarding fracture risk in hypoparathyroid patients treated with conventional therapy. A small cohort study of postmenopausal women noted an increase in morphometric vertebral fractures in patients with hypoparathyroidism treated with conventional therapy,[42] as did a cohort study in younger patients with idiopathic disease who had a high rate of anti-convulsant use.[43] Two registry studies failed to show an increase in overall fracture risk in hypoparathyroidism, although morphometric vertebral fractures were not assessed.[44,45] The significant improvement in lumbar spine BMD noted with rhPTH(1–84) therapy may be beneficial if there is indeed an increase in vertebral fracture risk. Given that failure load is a key predictor of incident fracture,[46] the effects of PTH therapy on fracture risk in hypoparathyroidism clearly deserve further study. Of note, no fractures occurred in our cohort during the study period.

We noted some significant relationships between age and cortical and trabecular parameters, consistent with other studies.[6,9,14,47] We did not note any relationships between gender or disease duration and any of the measured parameters in this study, which may be due to the relatively small sample size.

A final discussion point relates to the administration regimen of PTH. In this study, most of our patients were treated for most of the time with an every other day regimen of rhPTH(1–84). Against a backdrop of virtually absent PTH in these subjects, this rather unphysiological replacement regimen cannot be assumed to represent how PTH would affect the skeleton in hypoparathyroidism if a more physiological regimen were to have been available. We do not yet have a regimen that would provide replacement PTH in a manner that mimics tonic, circadian, and pulsatility dynamics that characterize the normal physiological state.

The strengths of this investigation include the uniquely large cohort of hypoparathyroid men and women followed through four years of continuous rhPTH(1–84) therapy using a noninvasive imaging technology not previously applied for this length of time to this disease state. Limitations include the inability to determine differences in response between pre- and postmenopausal women and men due to relatively small numbers per group. Another limitation is the pharmacologic replacement regimen of rhPTH(1–84) therapy used for this protocol. It remains to be seen whether more physiologic dosage regimens will show

different results. Finally, uncertainty in defining the subcomparmentalization of the cortical envelope awaits more sophisticated analyses.

Acknowledgments

This work was supported in part by NIH grants DK069350, DK32333 and DK095944 and Shire Pharma.

Funding source: NIH DK069350, DK095944, DK32333, Shire/Takeda

Disclosures: Dr. Cusano is a consultant for Radius and Shire/Takeda. Dr. Rubin receives research support from Shire/Takeda. Dr. Bilezikian is a consultant for Amgen, Radius, Ultragenyx, Regeneron, and Shire/Takeda.

References

1. Langdahl BL, Mortensen L, Vesterby A, Eriksen EF, Charles P. Bone histomorphometry in hypoparathyroid patients treated with vitamin D. Bone. 1996;18(2):103–8. [PubMed: 8833203]
2. Rubin MR, Dempster DW, Zhou H, et al. Dynamic and structural properties of the skeleton in hypoparathyroidism. J Bone Miner Res. 2008;23(12):2018–24. [PubMed: 18684087]
3. Rubin MR, Dempster DW, Sliney J Jr., et al. PTH(1–84) administration reverses abnormal bone-remodeling dynamics and structure in hypoparathyroidism. J Bone Miner Res. 2011;26(11):2727–36. [PubMed: 21735476]
4. Shoback D Clinical practice. Hypoparathyroidism. N Engl J Med. 2008;359(4):391–403. [PubMed: 18650515]
5. Shoback DM, Bilezikian JP, Costa AG, et al. Presentation of Hypoparathyroidism: Etiologies and Clinical Features. J Clin Endocrinol Metab. 2016 6;101(6):2300–12. [PubMed: 26943721]
6. Cusano NE, Nishiyama KK, Zhang C, et al. Noninvasive Assessment of Skeletal Microstructure and Estimated Bone Strength in Hypoparathyroidism. J Bone Miner Res. 2016;31(2):308–16. [PubMed: 26234545]
7. Rubin MR, Zhou H, Cusano NE, et al. The Effects of Long-term Administration of rhPTH(1–84) in Hypoparathyroidism by Bone Histomorphometry. J Bone Miner Res. 2018;33(11):1931–1939. [PubMed: 29972871]
8. Cusano NE, Rubin MR, McMahon DJ, et al. Therapy of hypoparathyroidism with PTH(1–84): a prospective four-year investigation of efficacy and safety. J Clin Endocrinol Metab. 2013;98(1):137–44. [PubMed: 23162103]
9. Macdonald HM, Nishiyama KK, Kang J, Hanley DA, Boyd SK. Age-related patterns of trabecular and cortical bone loss differ between sexes and skeletal sites: a population-based HR-pQCT study. J Bone Miner Res. 2011;26(1):50–62. [PubMed: 20593413]
10. Kreiger NTA, Joseph L, Mackenzie T, Poliqui S, Brown JP, Prior JC, Rittmaster RS. The Canadian Multicentre Osteoporosis Study (CaMos): background, rationale, methods. Can J Aging. 1999;18:376–87.
11. Burt LA, Liang Z, Sajobi TT, Hanley DA, Boyd SK. Sex- and Site-Specific Normative Data Curves for HR-pQCT. J Bone Miner Res. 2016;31:2041–2047. [PubMed: 27192388]
12. Boutroy S, Bouxsein ML, Munoz F, Delmas PD. In vivo assessment of trabecular bone microarchitecture by high-resolution peripheral quantitative computed tomography. J Clin Endocrinol Metab. 2005;90(12):6508–15. [PubMed: 16189253]
13. Laib A, Hauselmann HJ, Ruegsegger P. In vivo high resolution 3D-QCT of the human forearm. Technol Health Care. 1998;6(5–6):329–37. [PubMed: 10100936]
14. Khosla S, Riggs BL, Atkinson EJ, et al. Effects of sex and age on bone microstructure at the ultradistal radius: a population-based noninvasive in vivo assessment. J Bone Miner Res. 2006;21(1):124–31. [PubMed: 16355281]
15. Boutroy S, Vilayphiou N, Roux JP, et al. Comparison of 2D and 3D bone microarchitecture evaluation at the femoral neck, among postmenopausal women with hip fracture or hip osteoarthritis. Bone. 2011;49(5):1055–61. [PubMed: 21856461]

16. Burghardt AJ, Buie HR, Laib A, Majumdar S, Boyd SK. Reproducibility of direct quantitative measures of cortical bone microarchitecture of the distal radius and tibia by HR-pQCT. Bone. 2010;47(3):519–28. [PubMed: 20561906]
17. van Rietbergen B, Weinans H, Huiskes R, Odgaard A. A new method to determine trabecular bone elastic properties and loading using micromechanical finite-element models. J Biomech. 1995;28(1):69–81. [PubMed: 7852443]
18. Macneil JA, Boyd SK. Bone strength at the distal radius can be estimated from high-resolution peripheral quantitative computed tomography and the finite element method. Bone. 2008;42(6):1203–13. [PubMed: 18358799]
19. MacNeil JA, Boyd SK. Improved reproducibility of high-resolution peripheral quantitative computed tomography for measurement of bone quality. Med Eng Phys. 2008;30(6):792–9. [PubMed: 18164643]
20. Pistoia W, van Rietbergen B, Lochmuller EM, Lill CA, Eckstein F, Ruegsegger P. Estimation of distal radius failure load with micro-finite element analysis models based on three-dimensional peripheral quantitative computed tomography images. Bone. 2002;30(6):842–8. [PubMed: 12052451]
21. R Core Team. R: A Language and Environment for Statistical Computing. R Foundation for Statistical Computing 2018 Vienna, Austria ambs://www.R-project.org/
22. Rubin MR, Sliney J Jr, McMahon DJ, et al. Therapy of hypoparathyroidism with intact parathyroid hormone. Osteoporos Int. 2010;21(11):1927–34. [PubMed: 20094706]
23. Abugassa S, Nordenstrom J, Eriksson S, Sjoden G. Bone mineral density in patients with chronic hypoparathyroidism. J Clin Endocrinol Metab. 1993;76(6):1617–21. [PubMed: 8501170]
24. Chan FK, Tiu SC, Choi KL, Choi CH, Kong AP, Shek CC. Increased bone mineral density in patients with chronic hypoparathyroidism. J Clin Endocrinol Metab. 2003;88(7):3155–9. [PubMed: 12843159]
25. Laway BA, Goswami R, Singh N, Gupta N, Seith A. Pattern of bone mineral density in patients with sporadic idiopathic hypoparathyroidism. Clin Endocrinol (Oxf). 2006;64(4):405–9. [PubMed: 16584512]
26. Sikjaer T, Rejnmark L, Rolighed L, Heickendorff L, Mosekilde L. The effect of adding PTH(1–84) to conventional treatment of hypoparathyroidism: a randomized, placebo-controlled study. J Bone Miner Res. 2011;26(10):2358–70. [PubMed: 21773992]
27. Gafni RI, Brahim JS, Andreopoulou P, et al. Daily parathyroid hormone 1–34 replacement therapy for hypoparathyroidism induces marked changes in bone turnover and structure. J Bone Miner Res. 2012;27(8):1811–20. [PubMed: 22492501]
28. Rubin MR, Cusano NE, Fan WW, et al. Therapy of Hypoparathyroidism With PTH(1–84): A prospective six year investigation of efficacy and safety. J Clin Endocrinol Metab. 2016;101(7):2742–50. [PubMed: 27144931]
29. Sundh D, Mellström D, Nilsson M, Karlsson M, Ohlsson C, Lorentzon M. Increased Cortical Porosity in Older Men With Fracture. J Bone Miner Res. 2015 9;30(9):1692–700. [PubMed: 25777580]
30. Alvarenga JC, Fuller H, Pasoto SG, Pereira RM. Age-related reference curves of volumetric bone density, structure, and biomechanical parameters adjusted for weight and height in a population of healthy women: an HR-pQCT study. Osteoporos Int. 2017 4;28(4):1335–1346. [PubMed: 27981337]
31. Sornay-Rendu E, Boutroy S, Duboeuf F, Chapurlat RD. Bone Microarchitecture Assessed by HR-pQCT as Predictor of Fracture Risk in Postmenopausal Women: The OFELY Study. J Bone Miner Res. 2017 6;32(6):1243–1251. [PubMed: 28276092]
32. McCalden RW, McGeough JA, Barker MB, Court-Brown CM. Age-related changes in the tensile properties of cortical bone. The relative importance of changes in porosity, mineralization, and microstructure. J Bone Joint Surg Am. 1993;75(8):1193–205. [PubMed: 8354678]
33. Burghardt AJ, Buie HR, Laib A, Majumdar S, Boyd SK. Reproducibility of direct quantitative measures of cortical bone microarchitecture of the distal radius and tibia by HR-pQCT. Bone. 2010;47(3):519–528. [PubMed: 20561906]

34. Tsai JN, Uihlein AV, Burnett-Bowie SM, et al. Effects of Two Years of Teriparatide, Denosumab, or Both on Bone Microarchitecture and Strength (DATA-HRpQCT study). J Clin Endocrinol Metab. 2016;101(5):2023–30. [PubMed: 26964731]
35. Cohen A, Dempster DW, Müller R, et al. Assessment of trabecular and cortical architecture and mechanical competence of bone by high-resolution peripheral computed tomography: comparison with transiliac bone biopsy. Osteoporos Int. 2010;21(2):263–73. [PubMed: 19455271]
36. Parisien M, Silverberg SJ, Shane E, et al. The histomorphometry of bone in primar hyperparathyroidism: preservation of cancellous bone structure. J Clin Endocrinol Metab. 1990;70(4):930–8. [PubMed: 2318948]
37. Stein EM, Silva BC, Boutroy S, et al. Primary hyperparathyroidism is associated with abnormal cortical and trabecular microstructure and reduced bone stiffness in postmenopausal women. J Bone Miner Res. 2013;28(5):1029–40. [PubMed: 23225022]
38. Vignali E, Viccica G, Diacinti D, et al. Morphometric vertebral fractures in postmenopausal women with primary hyperparathyroidism. J Clin Endocrinol Metab. 2009;94(7):2306–12. [PubMed: 19401378]
39. Turner CH. Biomechanics of bone: determinants of skeletal fragility and bone quality. Osteoporos Int. 2002;13(2):97–104. [PubMed: 11905527]
40. Bjornerem A, Bui QM, Ghasem-Zadeh A, Hopper JL, Zebaze R, Seeman E. Fracture risk and height: an association partly accounted for by cortical porosity of relatively thinner cortices. J Bone Miner Res. 2013;28(9):2017–26. [PubMed: 23520013]
41. Boivin G, Farlay D, Bala Y, Doublier A, Meunier PJ, Delmas PD. Influence of remodeling on the mineralization of bone tissue. Osteoporos Int. 2009;20(6):1023–6. [PubMed: 19340504]
42. Mendonca ML, Pereira FA, Nogueira-Barbosa MH, et al. Increased vertebral morphometric fracture in patients with postsurgical hypoparathyroidism despite normal bone mineral density. BMC Endocr Disord. 2013;13:1. [PubMed: 23286605]
43. Chawla H, Saha S, Kandasamy D, et al. Vertebral fractures and bone mineral density in patients with idiopathic hypoparathyroidism on long-term follow-up. J Clin Endocrinol Metab. 2017;102(1):251–258. [PubMed: 27813708]
44. Underbjerg L, Sikjaer T, Mosekilde L, Rejnmark L. Postsurgical hypoparathyroidism--risk of fractures, psychiatric diseases, cancer, cataract, and infections. J Bone Miner Res. 2014;29(11):2504–10. [PubMed: 24806578]
45. Underbjerg L, Sikjaer T, Mosekilde L, Rejnmark L. The Epidemiology of Non-Surgical Hypoparathyroidism in Denmark: A Nationwide Case Finding Study. J Bone Miner Res. 2015;30(9):1738–44. [PubMed: 25753591]
46. Samelson EJ, Broe KE, Xu H, et al. Cortical and trabecular bone microarchitecture as an independent predictor of incident fracture risk in older women and men in the Bone Microarchitecture International Consortium (BoMIC): a prospective study. Lancet Diabetes Endocrinol. 2019;7(1):34–43. [PubMed: 30503163]
47. Dalzell N, Kaptoge S, Morris N, et al. Bone micro-architecture and determinants of strength in the radius and tibia: age-related changes in a population-based study of normal adults measured with high-resolution pQCT. Osteoporos Int. 2009;20(10):1683–94. [PubMed: 19152051]

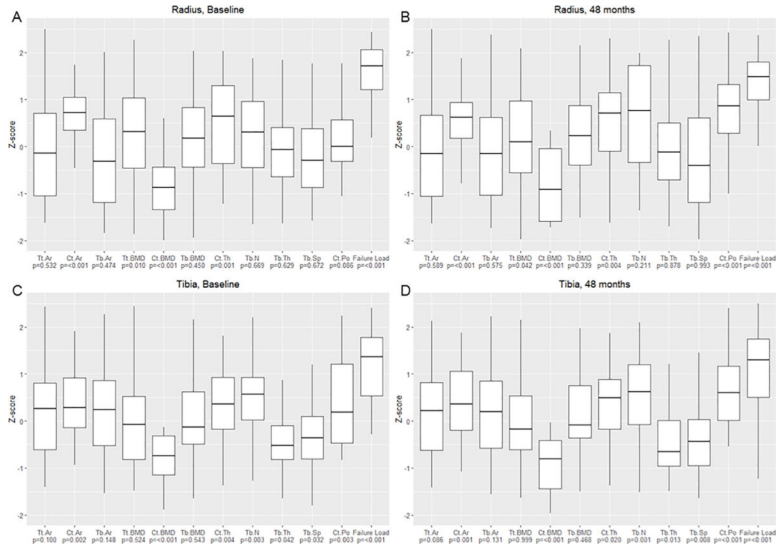

Figure 1.

Baseline and 48 month Z-scores for HRpQCT parameters in the hypoparathyroid cohort compared to normative controls from the Canadian Multicentre Osteoporosis Study [11] at the radius (baseline, panel A, and 48 months, panel B) and tibia (baseline, panel A, and 48 months, panel B). Median ± interquartile range.*$p<0.05$ compared with normative data; $^{\dagger}p<0.01$ compared with normative data; $^{\ddagger}p<0.001$ compared with normative data

Tt.Ar, total area; Ct.Ar, cortical area; Tb.Ar, trabecular area; Tt.BMD, total volumetric bone mineral density; Ct.BMD, cortical volumetric bone mineral density; Tb.BMD, trabecular volumetric bone mineral density; Ct.Th, cortical thickness; Tb.N, trabecular number; Tb.Th, trabecular thickness; Tb.Sp, trabecular separation; Ct.Po, cortical porosity

Table 1.

Baseline demographics, laboratory values, and bone density by dual energy X-ray absorptiometry for the hypoparathyroid cohort.

	Cohort (n=33)	Range*
Age (years), mean ± SD	47 ± 14	26–72
Gender, n **Women (premenopausal)** **Women (postmenopausal)** **Men**	16 8 9	
Height (cm), mean ± SD	166.1 ± 8	144.9–185.4
Weight (kg), mean ± SD	79.1 ± 15	47.6–115.7
Body mass index (kg/m^2)	28.7 ± 6	18.6–43.0
Etiology of disease **Postoperative** **Idiopathic**	19 14	
Duration of disease (years), median (IQR)	6 (3, 17)	2–45
Calcium dose (mg), median (IQR)	1833 (1400, 2700)	0–11,000
Calcitriol dose (μg), median (IQR)	0.50 (0.50, 0.85)	0–3.00
Serum calcium (mg/dL), mean ± SD	8.7 ± 1.0	8.6–10.2
PTH (pg/mL), median (IQR)	<3 (<3, <3)	10–65
25-hydroxyvitamin D (ng/mL), median (IQR)	35.8 (25.4, 48.7)	30–100
Phosphate (mg/dL), mean ± SD	4.41 ± 0.78	2.7–4.5
Magnesium (md/dL), mean ± SD	1.80 ± 0.16	1.5–2.5
Alkaline phosphatase (U/L), mean ± SD	64.4 ± 15	33–96

*Cohort range for demographic variables and normal reference range for laboratory variables

Table 2.

Percentage change in bone density by dual energy X-ray absorptiometry in the hypoparathyroid cohort through four years of rhPTH(1–84) therapy.

	Baseline (g/cm^2)	Baseline T-score	Baseline Z-score	12 months	24 months	48 months
Lumbar spine	1.219 ± 0.18	+1.3 ± 1.6	**+1.8 ± 1.5**$^{\wedge}$	0.0 ± 0.9%	**+2.7 ± 0.9%**†	**+4.9 ± 0.9%**‡
Femoral neck	0.962 ± 0.19	+0.8 ± 1.7	**+1.4 ± 1.5**$^{\wedge}$	−0.4 ± 0.9%	0.0 ± 0.9%	**+2.4 ± 0.9%***
Total hip	1.091 ± 0.18	+1.0 ± 1.3	**+1.4 ± 1.2**$^{\wedge}$	−1.4 ± 0.8%	**−2.1 ± 0.8%***	**−2.3 ± 0.8%**†
1/3 radius	0.731 ± 0.07	+0.2 ± 0.9	**+0.9 ± 1.0**$^{\wedge}$	**−1.8 ± 0.7%***	−0.1 ± 0.7%	+1.0 ± 0.7%
Ultradistal radius	0.482 ± 0.06	+0.3 ± 0.7	**+0.8 ± 0.9**$^{\wedge}$	**−1.5 ± 0.7%***	−1.2 ± 0.7%	**−2.1 ± 0.7%**†

Mean ± SD for baseline parameters; mean ± SEM for percentage change over time

$^{\wedge}$p<0.001 compared to healthy controls

*p<0.05 compared with baseline

†p<0.01 compared with baseline

‡p<0.001 compared with baseline

Table 3.

Baseline high resolution peripheral quantitative computed tomography parameters at the radius and tibia in the hypoparathyroid cohort and percentage change through four years of rhPTH(1–84) therapy, with baseline and 48 month Z-scores[Δ].

	Baseline	Baseline Z-score	12 months	24 months	48 months	48 month Z-score
Radius						
Tt.Ar (mm^2)	292 ± 15	−0.14	+0.1 ± 0.3%	0.0 ± 0.3%	+0.2 ± 0.3%	−0.12
Ct.Ar (mm^2)	68 ± 3	**+0.83**[‡‡]	−0.8 ± 0.7%	−0.7 ± 0.7%	**−1.8 ± 0.7%**[*]	**+0.75**[‡‡]
Tb.Ar (mm^2)	223 ± 14	−0.17	+0.3 ± 0.4%	+0.1 ± 0.4%	+0.8 ± 0.4%	−0.14
Tt.BMD (mg HA/cm^3)	363 ± 14	**+0.73**[**]	−0.6 ± 0.7%	−1.3 ± 0.7%	**−2.9 ± 0.7%**[‡]	**+0.56**[**]
Ct.BMD (mg HA/cm^3)	905 ± 12	**−1.28**[‡‡]	−0.8 ± 0.7%	**−1.7 ± 0.7%**[*]	**−3.8 ± 0.7%**[‡]	**−2.13**[‡‡]
Tb.BMD (mg HA/cm^3)	175 ± 9	+0.14	+0.9 ± 0.8%	+0.3 ± 0.8%	+0.8 ± 0.8%	+0.19
Ct.Th (mm)	1.09 ± 0.05	**+0.94**[††]	−0.7 ± 0.8%	−0.8 ± 0.8%	**−1.7 ± 0.8%**[*]	**+0.88**[††]
BV/TV (%)	0.146 ± 0.008	–	+0.9 ± 0.8%	+0.2 ± 0.8%	+0.8 ± 0.8%	-
Tb.N (1/mm)	2.07 ± 0.07	+0.11	+2.3 ± 1.8%	+0.7 ± 1.8%	+2.0 ± 1.8%	0.37
Tb.Th (mm)	0.071 ± 0.003	+0.10	−0.5 ± 1.6%	+0.2 ± 1.6%	−0.3 ± 1.6%	−0.03
Tb.Sp (mm)	0.431 ± 0.022	+0.11	−1.4 ± 1.8%	+0.1 ± 1.8%	−1.1 ± 1.8%	0.00
Tb.Sp.SD (mm)	0.188 ± 0.021	-	−1.8 ± 2.3%	−0.8 ± 2.3%	−2.5 ± 2.3%	-
Ct.Po (%)	1.7 ± 0.2	+0.39	+14.6 ± 17.7%	+33.2 ± 17.7%	**+88.5 ± 17.7%**[‡]	**+1.80**[‡‡]
Stiffness (N/mm)	60,633 ± 3,688	-	−0.4 ± 1.2%	−1.5 ± 1.2%	−1.6 ± 1.2%	-
Failure load (N)	2,476 ± 130	**+1.94**[‡‡]	−0.9 ± 1%	**−2.1 ± 1%**[*]	**−2.6 ± 1%**[*]	**+1.71**[‡‡]
	Baseline	**Baseline Z-score**	**12 months**	**24 months**	**48 months**	**48 month Z-score**
Tibia						
Tt.Ar (mm^2)	743 ± 25	+0.29	0.0 ± 0.3%	0.0 ± 0.3%	+0.5 ± 0.3%	+0.33
Ct.Ar (mm^2)	131 ± 5	**+0.57**[††]	0.0 ± 0.7%	+1.2 ± 0.7%	+0.5 ± 0.7%	**+0.63**[††]
Tb.Ar (mm^2)	611 ± 25	+0.27	+0.1 ± 0.4%	−0.2 ± 0.4%	+0.5 ± 0.4%	+0.29
Tt.BMD (mg HA/cm^3)	316 ± 9	+0.09	−0.5 ± 0.5%	−0.8 ± 0.5%	**−1.9 ± 0.5%**[‡]	0.00

	Baseline	Baseline Z-score	12 months	24 months	48 months	48 month Z-score
Ct.BMD (mg HA/cm^3)	868 ± 12	**−1.69**‡‡	−1.1 ± 0.7%	**−2.2 ± 0.7%**†	**−4.4 ± 0.7%**‡	**−2.56**‡‡
Tb.BMD (mg HA/cm^3)	186 ± 6	+0.10	+0.4 ± 0.4%	+0.1 ± 0.4%	+0.5 ± 0.4%	+0.12
Ct.Th (mm)	1.42 ± 0.05	**+0.59**††	−0.3 ± 1.1%	+1.3 ± 1.1%	−1.1 ± 1.1%	**+0.54****
BV/TV (%)	0.155 ± 0.005	-	+0.5 ± 0.4%	+0.2 ± 0.4%	+0.6 ± 0.4%	-
Tb.N (1/mm)	2.05 ± 0.05	**+0.56**††	+2.0 ± 1.2%	−0.2 ± 1.2%	+1.8 ± 1.2%	**+0.67**††
Tb.Th (mm)	0.076 ± 0.002	**−0.32****	−1.0 ± 1.2%	+0.9 ± 1.2%	−0.7 ± 1.2%	**−0.38****
Tb.Sp (mm)	0.422 ± 0.012	**−0.29****	−1.4 ± 1.1%	+0.6 ± 1.1%	−1.2 ± 1.1%	**−0.36**††
Tb.Sp.SD (mm)	0.182 ± 0.007	-	−0.8 ± 1.5%	+2.0 ± 1.5%	−0.3 ± 1.5%	-
Ct.Po (%)	4.8 ± 0.4	**+0.72**††	+4.6 ± 4.8%	**+12.9 ± 4.8%**†	**+23.1 ± 4.8%**‡	**+1.40**‡‡
Stiffness (N/mm)	150,022 ± 6,116	-	−1.6 ± 0.9%	−1.7 ± 0.9%	**−2.7 ± 0.9%**†	-
Failure load (N)	6,185 ± 217	**+1.35**‡‡	−1.2 ± 0.8%	−1.2 ± 0.8%	**−2.2 ± 0.8%**†	**+1.17**‡‡

$^{\Delta}$Compared to reference data from Canadian Multicentre Osteoporosis Study [11]

Tt.Ar, total area; Ct.Ar, cortical area; Tb.Ar, trabecular area; Tt.BMD, total volumetric bone mineral density; Ct.BMD, cortical volumetric bone mineral density; Tb.BMD, trabecular volumetric bone mineral density; Ct.Th, cortical thickness; BV/TV, trabecular bone volume; Tb.N, trabecular number; Tb.Th, trabecular thickness; Tb.Sp, trabecular separation; Tb.Sp.SD, trabecular heterogeneity; Ct.Po, cortical porosity

Mean ± SEM

*p<0.05 compared with baseline

†p<0.01 compared with baseline

‡p<0.001 compared with baseline

**p<0.05 compared with normative data

††p<0.01 compared with normative data

‡‡p<0.001 compared with normative data